Hydrophobic Coating of Silicate Phosphor Powder Using Atmospheric Pressure Dielectric Barrier Discharge Plasma

Quang Hung Trinh, Sang Baek Lee, and Young Sun Mok
Dept. of Chemical and Biological Engineering, Jeju National University, Jeju 690-756, Republic of Korea

DOI 10.1002/aic.14356
Published online January 16, 2014 in Wiley Online Library (wileyonlinelibrary.com)

A stable superhydrophobic coating was successfully deposited on commercial silicate-based orange phosphor by using atmospheric pressure dielectric barrier discharge plasma with hexamethyldisiloxane (HMDSO) and HMDSO/toluene mixture as precursors. Owning to the good optical properties, the deposited film acts not only as a hydrophobic protective layer but also as an antireflection optical thin film capable of improving the phosphor photoluminescence efficiency. The plasma-polymerized film based on Si—O—Si backbone containing methyl and phenyl nonpolar functional groups exhibited high-water-repellent characteristics. It was found that the water contact angle gradually increased with increasing the aging time and remained unchanged at about 140° after 1-month aging. Besides, the thermal stability of the coated phosphor under high-temperature condition was substantially enhanced by the aging. The findings of this work can contribute to improving the durability and reliability of the phosphor, eventually the long-term stability of phosphor-based light emitting diodes in practical applications. © 2014 American Institute of Chemical Engineers *AIChE J*, 60: 829–838, 2014

Keywords: hydrophobic coating, phosphor, plasma, dielectric barrier discharge, aging

Introduction

Phosphor is one of the key materials in light-emitting diode (LED)-based solid-state lighting technologies, which plays an important role in determining the performance of white LEDs, such as luminous efficacy, color rendering, correlated color temperature, color gamut, lifetime, and so forth.[1] Due to the presence of polar covalent chemical bonds, the photoluminescent phosphors exhibit hydrophilic character, that is, a tendency to interact with water or other polar substances. Recently, much attention has been paid to the durability enhancement of phosphor materials through hydrophobic (water-repellent) coating as the application fields of LEDs expand. The hydrophobic coating on phosphor materials possesses some obvious advantages, such as stable light emission, better humidity tolerance, and long-term stability. Up to now, a lot of research has been carried out to prepare self-cleaning stable hydrophobic surfaces, including chemical vapor deposition, dry particle coating, sol-gel process, atomic layer deposition, and plasma process.[2–6]

Plasma techniques can provide a good solution for hydrophobic layer deposition onto various substrates, keeping the bulk properties unchanged.[7–9] Besides, specific properties, such as hydrophobicity, optical characteristics, and layer thickness, can easily be controlled to desired levels using different precursor gases and appropriate plasma parameters. Even though a variety of plasma techniques are available for hydrophobic coating, atmospheric pressure plasmas, such as dielectric barrier discharge (DBD) and microwave discharge, are advisable because of drawbacks like the high cost of vacuum equipment and the space limitations that are frequently encountered in low-pressure plasma processes.[10] Especially, atmospheric pressure DBD adopted in this work is regarded as an effective and flexible method as it has many advantages over conventional vacuum-based plasmas. The use of atmospheric pressure allows expensive vacuum equipment to be eliminated and eases the incorporation of a plasma treatment into industrial production lines.[11] The DBD plasma has widely been applied for the generation of ozone; in ultraviolet (UV) sources and excimer lamps; in polymer treatment (particularly to enhance wettability, printability, and adhesion); for biological and medical applications; in CO_2 laser; in plasma-assisted combustion; and so on.[12–14] Above all, the surface treatment by plasma has attracted much attention of researchers in material processing fields because of its convenience, effectiveness, and low cost.

Plasma polymerization is used for the deposition of thin films on diverse substrates, as it yields layers which are generally amorphous, free of pinholes, highly cross-linked, highly resistant to heat, and corrosion and very adhesive to different substrates.[15] Topala et al.[9] obtained stable hydrophobic polystyrene films deposited onto glass and silicon substrates by using DBD plasma. Successful plasma polymerization of a fluorocarbon compound using an atmospheric pressure plasma jet was achieved by Vogelsang et al.[16] Although many articles dealing with plasma-mediated hydrophobic coating onto various substrates, such as glass, silicon, wood, and fabric, are reported, the applications of plasma processes, especially atmospheric pressure plasmas, to phosphor substrates are scarce in the literature. Lee et al.[7]

Correspondence concerning this article should be addressed to Y. S. Mok at smokie@jejunu.ac.kr.

Table 1. Properties of the Commercial Phosphor

Excitation Range (nm)	Peak Wavelength (nm)	Color Coordination		Average Particle Size (μm)
		CIEx	CIEy	
200 ~480	592.6 ± 1	0.5868	0.4117	15

investigated surface treatment of Y_2O_3:Eu phosphor for improving the hydrophobic property by using glow discharge plasma in a low-pressure environment of 1 Torr, who found that the plasma treatment significantly improved the hydrophobicity of the phosphors. As aforementioned, however, the main disadvantage of low-pressure plasmas is the necessity of vacuum systems. On the contrary, atmospheric pressure plasmas use relatively inexpensive and simple devices, and offer a simple way of obtaining hydrophobic surfaces using various precursor gases. Furthermore, atmospheric-pressure plasma processing can readily optimize the surface properties of substrates under a wide variety of treatment conditions since operating parameters of the reactor such as electric power, feed gas flow rate, and treatment time can all be adjusted independently from one another.

Having emerged as one of the most common precursors in a variety of applications, siloxanes possess many peculiar properties including good thermal stability, chemical resistance, tunable refractive index, tunable mechanical properties, and excellent photostability.[17] In addition, silicone-based polymers are highly transparent to UV, visible, and selected bands of near-infrared (IR) spectra.[18] Hexamethyldisiloxane (HMDSO), that is, a typical siloxane compound is nontoxic and does not produce any harmful compounds during processing. Thus, it can be used in production environment without any special safety considerations.[19] Plasma-mediated polymerization of the monomer HMDSO can yield both hard, hydrophilic SiO_x structures and soft, hydrophobic $SiO_xC_yH_z$ layers.[20]

In this work, we applied the atmospheric pressure DBD plasma to the deposition of organosilicon-based thin films from HMDSO and HMDSO/toluene mixture on a commercial silicate-based orange phosphor powder (Sr_2SiO_4:Eu^{2+}). The aim of this article is to prepare stable hydrophobic coating onto the phosphor substrate by plasma treatment at atmospheric pressure and ambient temperature. To achieve uniform coating of irregularly shaped phosphor powder, a rotary DBD plasma reactor consisting of a quartz tube and concentric metal electrodes was used. Characterizations of the plasma-polymerized thin films were performed by using various techniques, such as contact angle (CA) goniometer, photoluminescence (PL) spectroscopy, transmission electron microscopy (TEM), field emission scanning electron microscope (FE-SEM), x-ray diffraction (XRD) spectroscopy, and Fourier-transform infrared (FTIR) spectroscopy.

Experiments

Materials

Commercially available silicate-based orange phosphor (product name: PA602A1) with a peak wavelength of 592.6 nm and an average particle size of 15 μm was supplied by Force4 Co. Europium-activated strontium orthosilicate (Sr_2SiO_4:Eu^{2+}) is one of the promising candidates that can replace the most popular commercial phosphor, $Y_3Al_5O_{12}$:Ce^{3+} (YAG:Ce^{3+}).[21] The Sr_2SiO_4:Eu^{2+} phosphor has outstanding features, such as a broad range of emission spectra and fairly good optical transmission. Table 1 summarizes the details of the characteristics of Sr_2SiO_4:Eu^{2+}. The precursors including HMDSO and toluene for the preparation of hydrophobic coating were purchased from Sigma-Aldrich. In this work, argon was chosen as the carrier gas for evaporating and feeding HMDSO and toluene to the DBD plasma reactor.

Apparatus and methods

Plasma-mediated deposition of hydrophobic layer over the phosphor powder surface was carried out in a rotary DBD plasma reactor, referred to as plasma reactor. Figure 1 shows the schematic diagram of the principle components of the plasma reactor comprising a quartz tube (inner diameter: 22 mm; outer diameter: 25 mm), a high-voltage coaxial stainless steel electrode (diameter: 6 mm), and a copper coil electrode wound around the outside of the quartz tube. The stainless-steel electrode was fixed with two steel tubes at both ends. The feed gas containing the precursors (HMDSO and/or toluene) is introduced and exhausted through the holes made in the steel tubes. The effective reactor length that the plasma discharge occurred was about 120 mm. The volume of the plasma region was calculated to be 42.2 cm^3.

For the preparation of a uniform hydrophobic coating layer over the phosphor powder substrate, the plasma reactor was slowly rotated by an electric motor via a set of belt and pulley at a rate of 2.0 rev s^{-1}. The plasma reactor was energized by an alternating current (AC) voltage whose operating frequency was 60 Hz. As shown in Figure 1, the electrodes were connected to the AC power source via Y-type couplings for electrical contacts. The voltage waveforms were recorded using a 1000:1 high-voltage probe (PHV4–2934, LeCroy) and a digital oscilloscope (Wavejet 354A, LeCroy). The input power was monitored with a digital power meter (Power manager, DAWON DNS Co.). About 10 g of phosphor powder was put into the plasma reactor, and then plasma-treated at voltages from 19.3 to 24.2 kV (peak value). In this voltage range, the input power changed in the range of 20–30 W, tantamount to input power densities of 474–711 mW cm^{-3}. The precursors were vaporized and introduced to the plasma reactor by bubbling with known flow rates of argon carrier gas through liquid HMDSO and

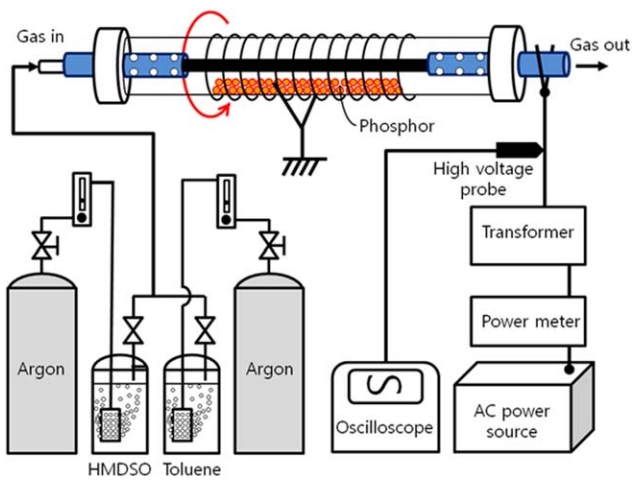

Figure 1. The schematic diagram of the experimental apparatus.

[Color figure can be viewed in the online issue, which is available at wileyonlinelibrary.com.]

toluene in glass containers. To ensure proper vaporization of HMDSO and toluene, ceramic gas diffusers capable of forming tiny bubbles were used. When HMDSO alone was used as the precursor, the flow rate of argon was 2.0 L min^{-1}. In HMDSO/toluene mixture case, the flow rate of argon for evaporating toluene was changed in the range of 0.5–1.5 L min^{-1} with that for evaporating HMDSO kept constant at 1.0 L min^{-1}. The temperature of HMDSO and toluene was kept at 15°C by a cooling water circulator. At this temperature, the vapor pressures of HMDSO and toluene are 3.3 and 2.2 kPa, respectively. The contents of HMDSO and toluene were calculated by their vapor pressures. The experimental variables were treatment time for coating, electric power delivered to the plasma reactor, and precursor composition. The plasma treatment time was varied in the range of 10–60 min in 10 min intervals. All experiments were conducted at room temperature.

Analyses and measurements

The hydrophobicity of the coating was probed by measuring static CA of water and glycerol. The CA measurements were carried out on a goniometer (SEO Phonix 300) using sessile drop technique by dropping about 10 μL of water or glycerol. In the present work, each CA value reported was the average of at least 10 measurements. The samples for CA measurements were prepared by spreading the phosphor powder onto double-sided tapes.

To examine the optical behavior, the PL spectra of the phosphor powder were measured by a fluorescence spectrophotometer (HITACHI F-4500) with a 1.0-nm resolution equipped with a 150 W Xe lamp as a light source at room temperature. The functional groups responsible for the hydrophobicity of the coating layer were identified by an FTIR spectrometer (NICOLET 6700). Since bare phosphor exhibited some broad strong absorbance bands which overlapped the weak ones of the coating layer in the wavenumber range of 400–4000 cm^{-1}, the FTIR spectra of the plasma-treated phosphors did not clearly show the characteristic peaks of the coating layer. To resolve this problem, 10-mm KBr disc, which is transparent to IR from 4000 to 400 cm^{-1}, was coated by the same procedure as above, and analyzed by the FTIR. The FTIR spectrum of the coated KBr disc clearly showed the characteristic bands of the deposited thin films.

To characterize the thin film layer and investigate its influences on the hydrophobic and optical behaviors, the plasma-treated phosphors were analyzed using a cross-sectional TEM (JEOL JEM-2000 FX II) operated at 200 kV with a resolution scanning of 1.5 nm. The morphology observation of the organosilicon-based thin films was carried out by a FE-SEM (JEOL JSM-6700F). To compare the crystalline structures before and after the plasma treatment, the XRD characterization was performed on a XRD system (D/MAX 2200H, Bede 200, Rigagu instruments).

Results and Discussion

Hydrophobic characteristics

Figure 2a shows the variations of water CA (WCA) as a function of plasma treatment time. During the plasma treatment, the decomposition of HMDSO precursor took place via the collisions with energetic species such as electrons and excited Ar molecules, and the fragments generated in

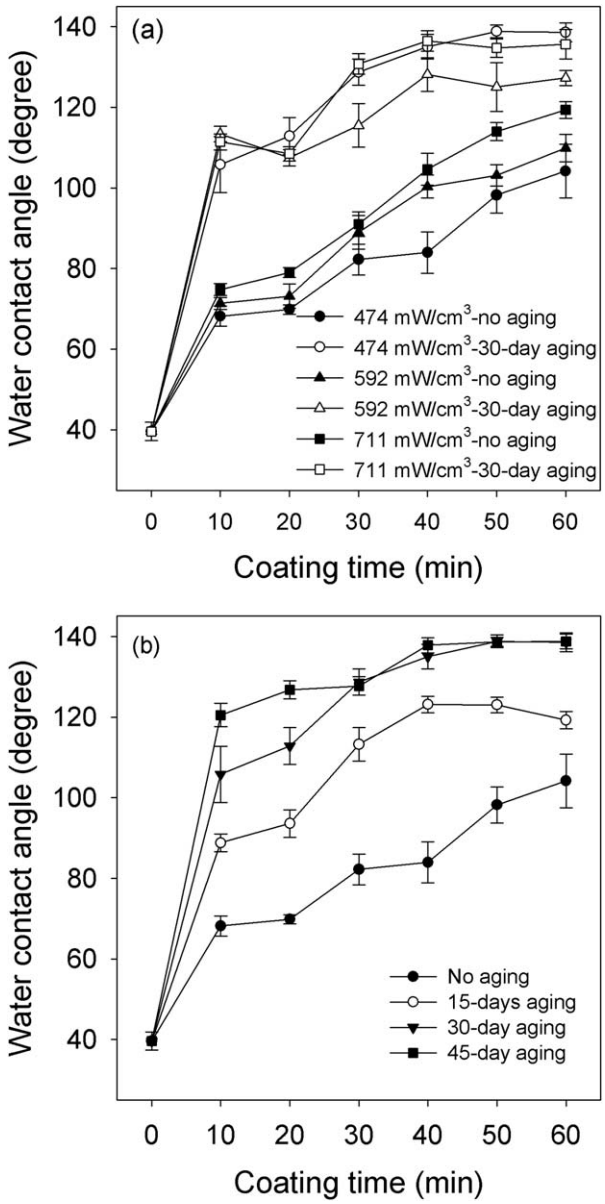

Figure 2. Variations of water contact angle (WCA) as a function of plasma treatment time at different input power densities (a), and the dependence of WCA on the aging time (b).

the plasma deposited on the surface of the phosphor to form thin hydrophobic layer. As expected, the WCA tended to gradually increase with increasing the treatment time due to the increase in the hydrophobicity. When compared at identical treatment time, say, at 60 min, higher electric power resulted in larger WCA, which is obviously because the decomposition of HMDSO was enhanced, in turn facilitating the deposition of the fragments on the powder surface. As can be seen, the WCAs measured right after 60-min treatments were 104°, 110°, and 119° at input power densities of 474, 592, and 711 mW cm^{-3}, respectively. Interestingly, remarkable increases in the WCA were observed after aging the plasma-treated phosphor for 30 days. In this work, the plasma-treated phosphor powder samples were stored in glass-sealed bottles for aging at room temperature. Contrary to our expectation, the samples aged for 30 days revealed larger WCAs that those without aging. This result may be

explained by a phenomenon known as hydrophobic recovery of hydrophilic treatment. The driving force for the hydrophobic recovery is the thermodynamic requirement of minimizing the surface free energy. Reorientation of polar groups at the surface into the bulk and migrations of low-molecular mass (LMM) components to the surface are believed to be dominant mechanisms for the enhancement of hydrophobicity. The polar functional segments may experience repulsive forces at the polymer layer/air interface and be reorientated inwards. Natural diffusion process is responsible for the movement of LMM components from inner bulk to topmost surface. The more the LMM components on the surface, the larger its hydrophobicity and vice versa.[22–25]

To understand more about the effect of the aging on the WCA, the aging time was changed up to 45 days, and the results are presented in Figure 2b. So as to compare the WCAs on identical basis, the plasma treatment of the phosphor powder was conducted at an input power density of 474 mW cm^{-3}. As observed, the samples aged after the plasma treatment exhibited larger WCAs. After 15 days of aging, the WCA increased by 15°–40°, as compared to the cases without aging. Particularly, the samples aged for 30–45 days showed the transition from hydrophobic to superhydrophobic state. Based on 50–60 min coating time, maximum WCA of about 140° was observed for the phosphor samples aged for 30 and 45 days. It appears that the WCA remained unchanged after 1-month aging, implying that the hydrophobicity became stable.

To investigate the thermal stability of the coating, the phosphor samples prepared with the HMDSO precursor at an input power density of 474 mW cm^{-3} (coating time: 40 min) were annealed in air at various temperatures for 10 min. Figure 3a shows the effect of the annealing temperature on the WCA, where two cases of 3-day and 33-day aging time are compared. Although the WCA of the 3-day-aged sample kept increasing with increasing the annealing temperature, that of the 33-day-aged sample remained unchanged at 133° at annealing temperatures from 10 to 110°C, and slightly increased by further increases in the annealing temperature up to 210°C. This phenomenon may be explained by the facilitation of the migration of LMM components from the bulk to the topmost surface of the coating layer at high temperatures. Since the 3-day-aged sample obviously contained more LMM components in the bulk, the increase in the WCA resulting from the annealing process was more noticeable. Figure 3b presents the WCAs obtained by changing the annealing time up to 60 min with the annealing temperature kept constant at 160°C. Starting with a rapid increase for the first 40 min, the WCA of the 3-day-aged sample slightly decreased with further increasing the annealing time. Conversely, the 33-day-aged sample revealed a good thermal stability. The coating layer would complete the spontaneous restructuring process and become stable if sufficient aging time is provided. It is worthwhile to note that the WCA and therefore the hydrophobic characteristics of the coating have significantly been enhanced instead of being degraded with the natural aging and thermal treatment, suggesting that the coated phosphor can be useful for phosphor-based devices working under harsh conditions or in exterior applications.

Figure 4 depicts the WCA and glycerol CAs (GCA) measured right after the plasma treatment of the phosphor powder. The precursor was HMDSO and the input power density

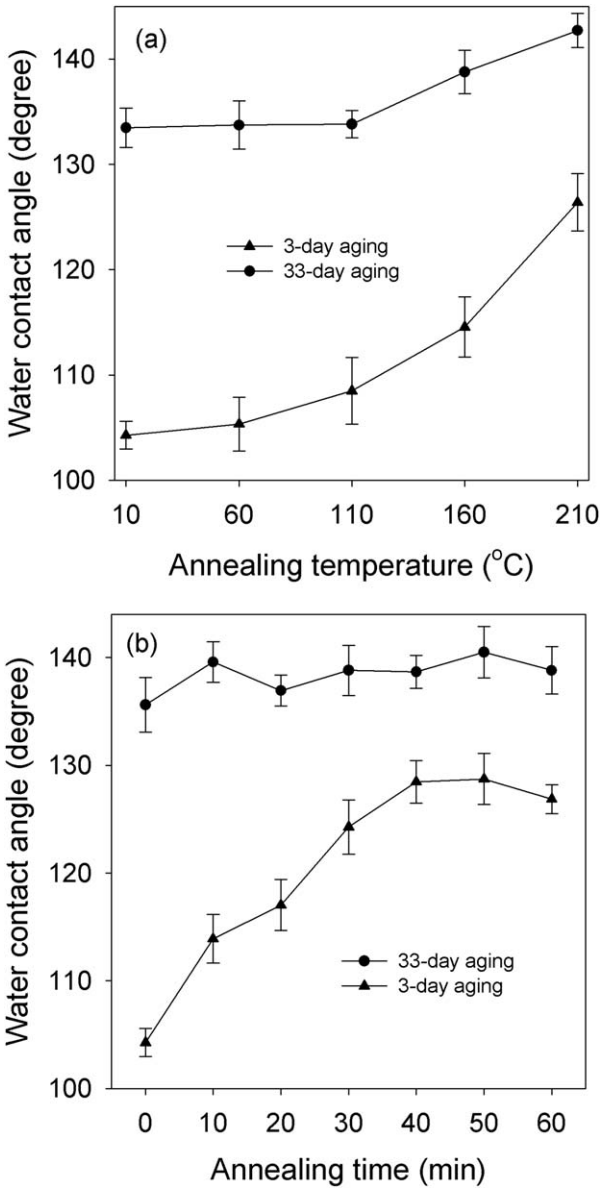

Figure 3. Effect of the annealing temperature (a) and the annealing time (b) on the water contact angle.

for creating plasma was 711 mW cm^{-3}. As discussed above, it is natural that larger CAs should be observed at longer treatment time for both glycerol and water. The GCA was considerably higher than the WCA at the same treatment time due to the weaker interaction with the sample surface. From CAs of these liquids, the surface free energy can be calculated. The surface free energy is an important characteristic of the coating to estimate the wettability. To determine the surface free energy using Owens–Wendt theory, CA measurements with at least two different liquids are necessary.[26] The relation between the CA and the surface free energy is as follows

$$\gamma_L(1+\cos\theta)=2\left(\sqrt{\gamma_S^d\cdot\gamma_L^d}+\sqrt{\gamma_S^P\cdot\gamma_L^P}\right) \quad (1)$$

where γ_s^d and γ_s^p are dispersive and polar components of the surface energy of the solid surface, γ_L^d and γ_L^p are dispersive and polar components of the surface energy of the testing

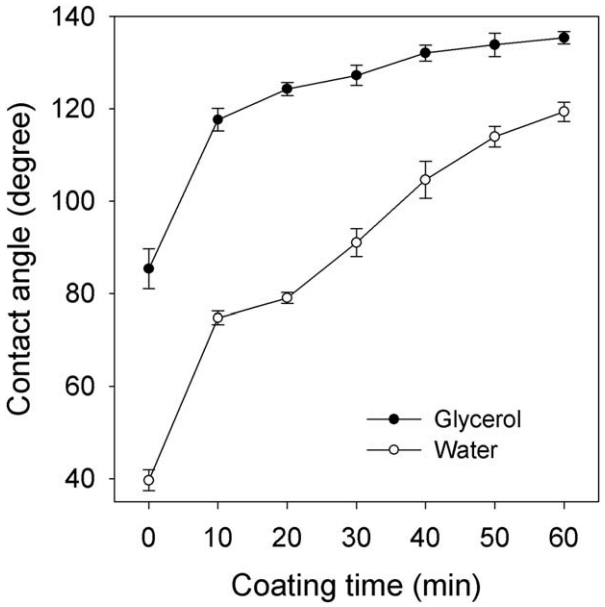

Figure 4. Comparison between water contact angle and glycerol contact angle.

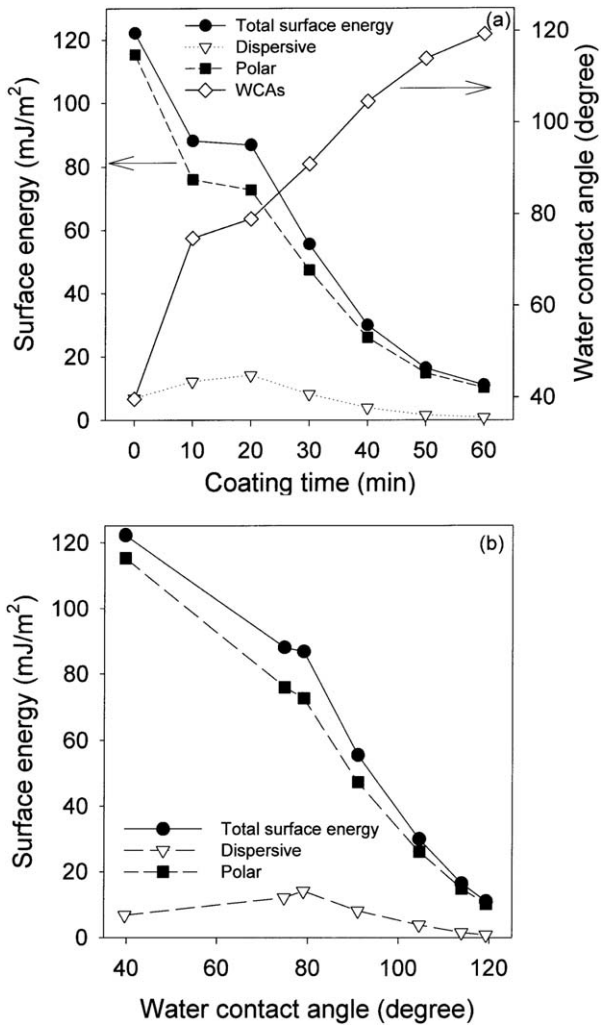

Figure 5. Surface free energy as a function of plasma treatment time (a), and as a function of water contact angle (b).

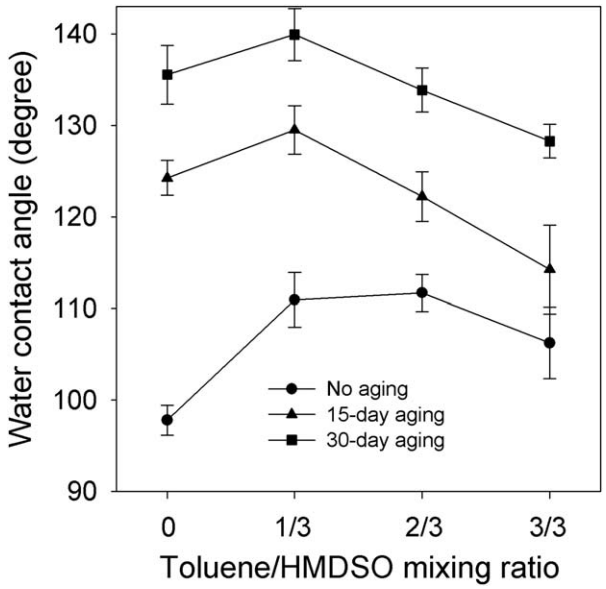

Figure 6. Dependence of water contact angle on the toluene/HMDSO ratio.

liquid, and θ is the CA. In the present work, we utilized the Surfaceware 7 software package adopting the aforementioned Owens–Wendt method. The surface energy was determined from the WCA and GCA measured right after the preparation of the coating. The surface energy obtained by the software is presented in Figure 5a as a function of the treatment time. Switching from hydrophilicity to hydrophobicity can also be observed in Figure 5a by the changes in the surface energy. For information, the WCAs were also shown in Figure 5a. The total surface energy, which consists of polar and dispersive components, rapidly decreased with increasing the coating time. After a slight increase from 6.9 to 14.2 mJ m^{-2} for the first 20 min, the dispersive component kept decreasing and ended at 0.8 mJ m^{-2}. Compared to the dispersive component, the polar one was much larger, which mainly constituted the total surface energy. It decreased from 115.3 to 10.2 mJ m^{-2} when the coating time increased from 0 to 60 min. The surface energy data in Figure 5a were replotted against the WCA (Figure 5b), which shows that the total surface energy decreased almost linearly with the WCA.

The hydrophobicity of the phosphor powder may be further improved by using toluene as a coprecursor, as demonstrated by Lee et al.[7] The dependence of WCA on the toluene/HMDSO ratio is shown in Figure 6. With keeping the coating time at 40 min, the input power density at 711 mW cm^{-3} and the argon flow rate for evaporating HMDSO at 1.0 L min^{-1}, the argon flow rate for evaporating toluene was varied up to 1.5 L min^{-1}. Just like the HMDSO-alone case, the WCA measurements were carried out right after the plasma treatment and after aging for some time. All three cases, that is, without aging, 15-day aging and 30-day aging, showed similar behavior in the WCA, even though the WCA values were different from one another. The WCA of the sample without aging evidently increased from 98° to 111° when the toluene/HMDSO ratio increased from 0 to 1/3. Similar trend was also observed for the 15-day-aged and 30-day-aged samples. However, the WCA tended to decrease with increasing the toluene/HMDSO ratio to 2/3 and 3/3. The best WCA was observed at the toluene/HMDSO ratio of

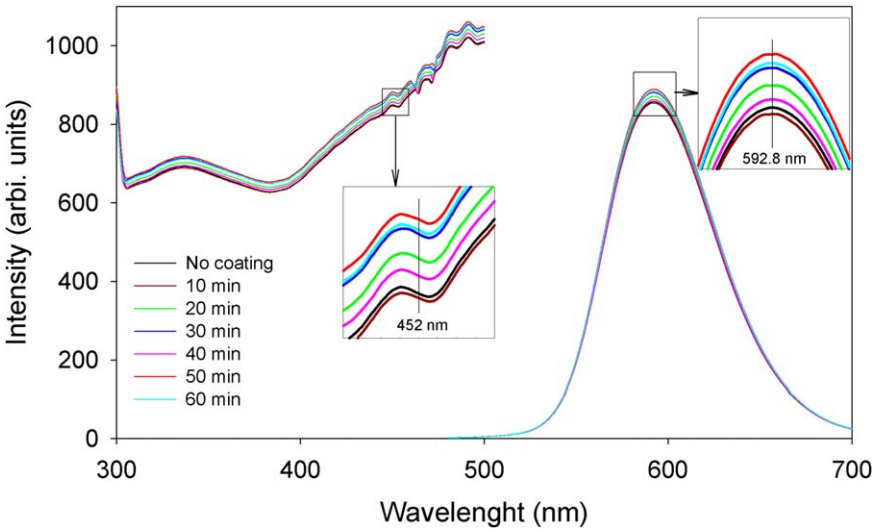

Figure 7. Photoluminescence spectra of the phosphor with and without hydrophobic coating.

[Color figure can be viewed in the online issue, which is available at wileyonlinelibrary.com.]

1/3 for all three cases. The optimum value of the toluene/HMDSO ratio observed here is consistent with the results reported by Lee et al.[7] At this toluene/HMDSO ratio, the WCAs of the 15-day-aged and 30-day-aged samples were measured to be 130 and 140°, respectively.

Optical properties

Besides CA and surface energy, the PL also plays a key role in determining the quality of the phosphor. The PL and excitation spectra of the phosphors with and without hydrophobic coating are shown in Figure 7 as a function of plasma treatment time. The preparation of the hydrophobic coating was performed with HMDSO at an input power density of 474 mW cm^{-3}, and then aged for 30 days. As can be seen, the coating not only promoted the hydrophobic characteristics, but also affected the PL spectra because the coating layer affected the excitation of the phosphor and the emission of photons. The Eu^{2+} ions in the ground state are excited to higher electronic states by absorbing energy from the excitation source; then, the so-called "Stokes shift" occurs. The silicate phosphor of this work showed a wide excitation band located at around 380 nm. The wide excitation band indicates that the phosphor is well-excited by near-UV light. The emission band was observed to be quite broad, centered around 592.8 nm, which is attributed to a strong coupling interaction between the Eu^{2+} ions and the Sr_2SiO_4 host matrix.[27] The intensity changes in the emission spectra had a similar pattern to those in the excitation spectra, suggesting that the excitation energy mainly affected the emission energy. In other words, the more the excitation energy delivered to the phosphor, the more the emission energy. Letting the emission intensity of the bare phosphor be 100%, relative emission intensities of the plasma-treated samples were estimated and tabulated in Table 2. Even though some fluctuations were observed, increasing tendency according to the plasma treatment time was exhibited. It is noteworthy that the emission intensity obtained at 50-min treatment increased by 3.74% and there was no change in peak wavelength. Such an improvement in the PL intensity due to the presence of the coating layer may be interpreted as follows. As depicted in Figure 8, if the optical thickness of the coating film is equal to 1/4 of the wavelength of the incident monochromatic light, and the index of refraction of the film is the square root of the material on the surface of which the film has been deposited, the reflections from the surface and the interface are out of phase and completely cancel one another,[28] that is, there is zero reflection of the monochromatic light. The optical thickness of the film can be calculated from the phase difference between two light waves reflected from surfaces of the film

$$\Delta\phi = \frac{2\pi L}{\lambda} \tag{2}$$

where $\Delta\phi$ is the phase difference, L is the optical path length, $L = 2t$ (t: optical thickness of the film), and λ is the wavelength of the incident light. The destructive interference occurs when the phase difference is

$$\Delta\phi = \frac{2\pi L}{\lambda} = \frac{4\pi t}{\lambda} = \pi \tag{3}$$

Finally, we obtain

$$t = \frac{\lambda}{4} \tag{4}$$

In the absence of the coating layer, a part of the excitation light was reflected at the surface and a part passes through the crystal lattice of the phosphor. Conversely, in the presence of the coating layer, the excitation light was divided into three parts: reflection, absorption, and transmission. Although the reflection and absorption by the coating layer

Table 2. Peak Wavelengths and Relative Emission Intensities of the Phosphors Prepared with HMDSO

Coating Time (min)	0	10	20	30	40	50	60
Wavelength (nm)	592.8	592.8	592.6	592.4	592.2	592.8	592.4
Intensity (%)	100	99.61	101.59	102.81	100.61	103.74	103.05

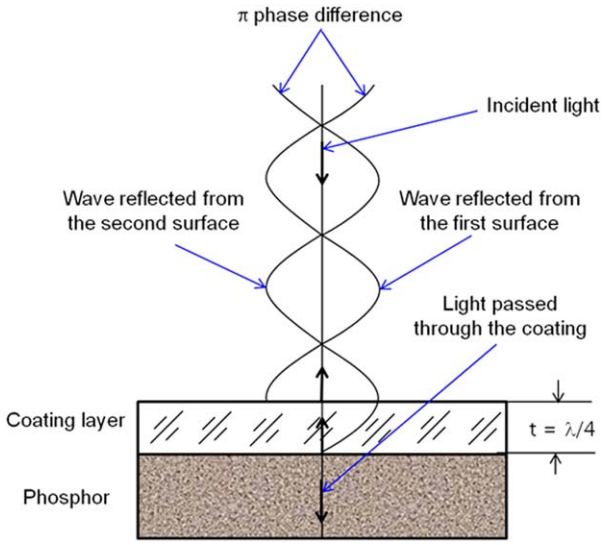

Figure 8. Optical behavior of the coated phosphor.

[Color figure can be viewed in the online issue, which is available at wileyonlinelibrary.com.]

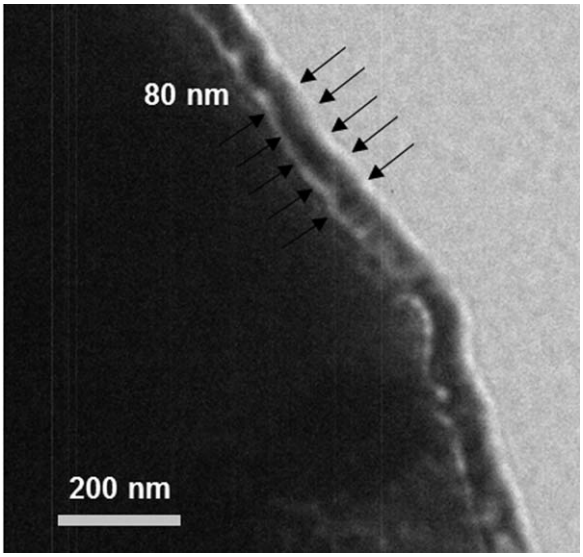

Figure 9. TEM image of the coated phosphor.

did not reach into the phosphor crystal lattice, the last one was responsible for the radiative transition, being partially converted into visible light. In Figure 7, the improvement in the excitation intensity as a result of the coating indicates that the reflection of the excitation light was perceptibly reduced, that is, after the preparation of the coating layer, more excitation energy was delivered into the phosphor lattices. Assuming that the deposited thin film of the 50-min-treated sample has the lowest reflection of the excitation light at 500 nm wavelength, the optical thickness (t) of the thin film should be $\lambda/4 = 125$ nm from Eq. 4. The physical thickness (d) of the coating film was measured to be about 80 nm by the TEM analysis (see Figure 9 below). The refractive index (n) of the film is given by

$$n = \frac{t}{d} \tag{5}$$

Thus, the refractive index is calculated to be 1.56 at the wavelength of 500 nm. The refractive index of HMDSO-based coating is generally ranges from 1.40 to 1.57 at 589 nm.[29] The refractive index calculated here agrees well with the reported value. From Figure 7, one can also observe that the excitation intensity considerably increased for the 50-min-treated sample at 452 nm which is typical radiation wavelength of blue LED chips, suggesting that the preparation of the coating is advisable for improving phosphor-based LEDs. Meanwhile, the emission intensities of the samples obtained by using the HMDSO/toluene precursor were also higher than the bare phosphor. For example, at toluene/HMDSO ratios of 1/3 and 3/3, the PL of the 30-day aged samples increased by 2.4 and 3.6%, respectively, indicating that the presence of the phenyl group due to toluene did not nearly affect the PL. The chemical composition of the coating layer will be discussed further.

Surface morphology

The structure and morphology of the thin hydrophobic film were investigated using TEM, SEM, and XRD. The TEM image of the phosphor sample after the preparation of the coating at an input power density of 474 mW cm^{-3} for 50 min is shown in Figure 9. The thin film was a uniform single-layer with a thickness of approximately 80 nm. Even though the concentration of the precursor decreases along

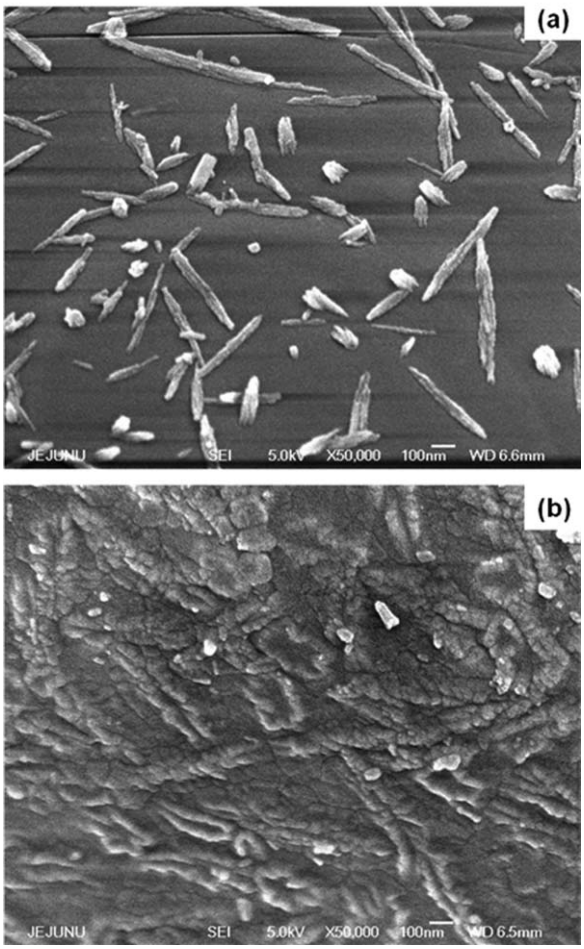

Figure 10. SEM images of the phosphor surfaces before and after the preparation of the coating.

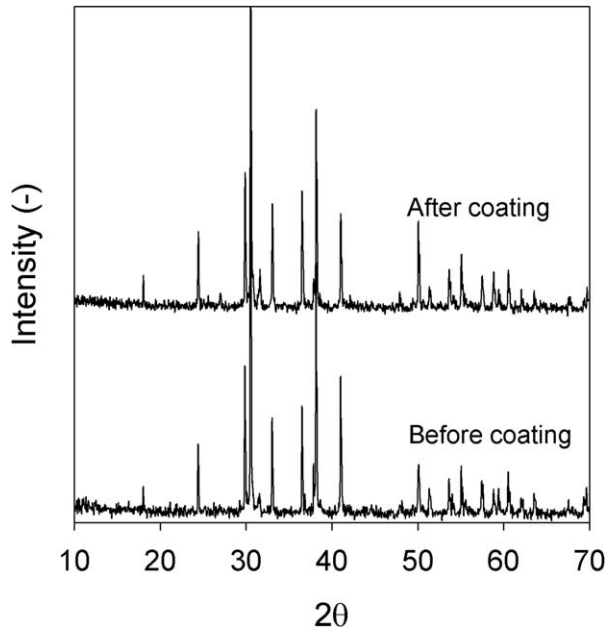

Figure 11. XRD patterns of the phosphors before and after the preparation of the coating.

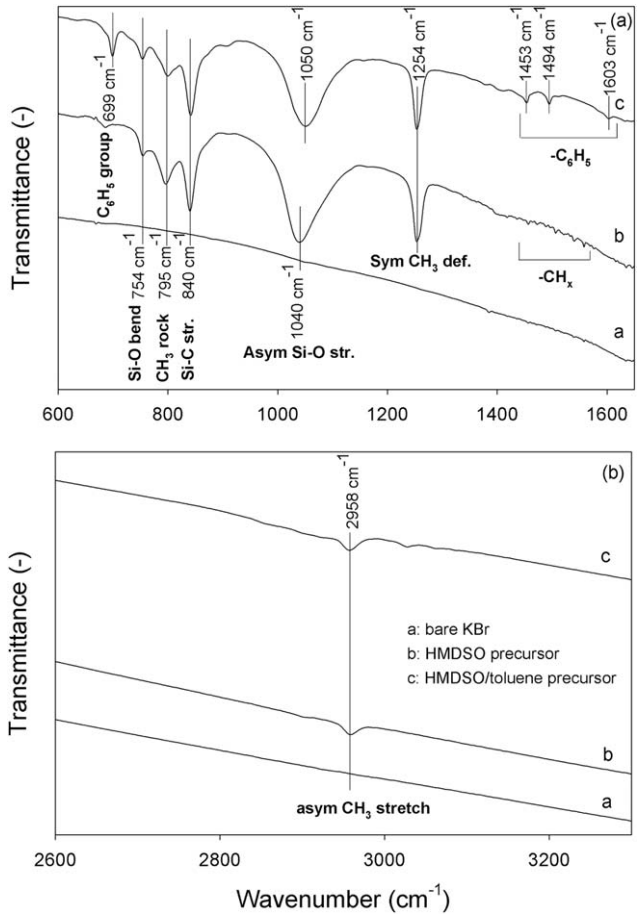

Figure 12. FTIR spectra of the KBr discs coated with HMDSO and HMSO/toluene mixture in spectral range of 400–1650 cm^{-1} (a) and 2600–3300 cm^{-1} (b).

the stream in plasma zone, it can be said that the coating thickness is uniform throughout the reactor. Note that the precursor was fed in excess to the plasma reactor, resulting in negligible concentration difference between the inlet and outlet of the reactor. According to the FTIR gas analysis, the concentration of the precursor (HMDSO) decreased from 31,500 ppm at the inlet to 29,900 ppm at the outlet when the input power density was 474 mW cm^{-3}. Figures 10a, b show the SEM images of the phosphor surfaces before and after the preparation of the coating, respectively. After the hydrophobic coating, the SEM image revealed a smooth surface morphology, indicating that the surface was well-covered by the coating layer. The formation of thin coating layer can reduce the surface defects to decrease the surface free energy, thereby, improving the PL intensity.

Figure 11 shows the XRD patterns of the bare and plasma-treated phosphor (input power density: 474 mW cm^{-3}; treatment time: 50 min). Despite the 80-nm-thick hydrophobic coating layer, the plasma-treated phosphor exhibited the same XRD pattern with the bare phosphor. This result is because the plasma-mediated hydrophobic coating is generally amorphous and its thickness is too thin to affect the XRD pattern of the phosphor powder substrate.

Chemical composition of the coating

The FTIR spectra of the KBr discs coated with HMDSO and HMSO/toluene mixture at an input power density of 474 mW cm^{-3} are shown in Figure 12a. As aforementioned, since some absorbance bands of the phosphor itself overlap those of the coating layer, IR-transparent KBr disc was used as the substrate. By this way, the functional groups responsible for the hydrophobicity can be identified. As can be seen, the FTIR spectra of both precursor cases revealed the formation of Si—O—Si backbone with nonpolar organic groups attached to silicon atoms. The coating layers prepared from the HMDSO and HMDSO/toluene mixture featured strong absorption bands at around 1040 and 1050 cm^{-1} that are associated with the asymmetric Si—O—Si stretching vibrations. The position and shape of the band are affected by the molecular weight of the relevant component and properties of the substituent groups,[30] which can explain the band shift from 1040 to 1050 cm^{-1}. Moreover, the Si-O bending in Si—O—Si at 754 cm^{-1} was also observed from the spectra. Another feature of the HMDSO- and HMDSO/toluene-deposited films is the presence of CH_3 group. Although the absorbance band at 795 cm^{-1} can be assigned to Si-CH_3 rocking vibration, the other ones at 840 and 1254 cm^{-1} can be attributed to the Si—C stretching vibrations in Si—CH_3 and CH_3 symmetric deformations in CH_3—Si—CH_3, respectively. In Figure 12b, the absorbance band at 2958 cm^{-1} can be ascribed to the CH_3 asymmetric stretching. The weak absorbance bands scattered between 1400 and 1500 cm^{-1} that appeared in the HMDSO-deposited film correspond to the formation of CH_x groups (Figure 12a). The HMDSO/toluene-deposited film is characterized by the bands (699, 1453, 1494, and 1603 cm^{-1}) associated with the phenyl (C_6H_5) group. The existence of the hydrophobic functional groups, such as methyl (—CH_3) and phenyl (—C_6H_5), is responsible for the water repellent properties of the coating layers. Retaining these groups suggests that the dissociation of the precursors mainly resulted from bond breaking of Si—C and Si—O in

HMDSO and C—C in toluene. Plausible plasma-chemical reactions are as follows

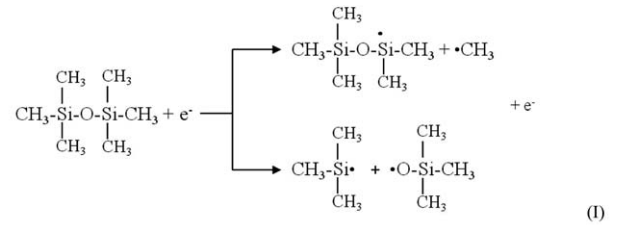

(I)

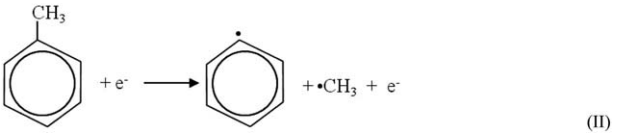

(II)

During plasma discharge, the ionizations of argon produced numerous energetic electrons which collided with precursor molecules, such as HMDSO and toluene. The reactive fragments generated from reactions I and II deposit on the phosphor powder surfaces to form thin hydrophobic layers. It should be noted that detailed reaction mechanisms are much more complicated since there are many possible reactions occurring simultaneously.

Conclusions

The formation of stable hydrophobic coating layer on the commercial silicate-based phosphor was achieved by using the atmospheric pressure rotary DBD plasma reactor with HMDSO and HMDSO/toluene mixture as the precursors. The increases in the input power density and the treatment time were observed to largely increase the hydrophobicity of the phosphor powder. The WCA measurements showed that the plasma treatment of the phosphor powder followed by aging led to superhydrophobic behavior of the surface, retaining good thermal stability. The hydrophobic coating also improved the PL intensity without a color shift as well as the excitation intensity. The surface morphology analyses including TEM, SEM, and XRD showed that the coating layer covering the phosphor powder surface is amorphous, uniform, and approximately 80-nm thick, acting as a low-reflection optical thin film in the excitation wavelength region. By the FTIR analyses, the deposited film is based on Si—O—Si backbone containing methyl and phenyl functional groups. The results of this work suggest that the preparation of the coating is advisable for improving phosphor-based LEDs.

Acknowledgment

This research was financially supported by the Ministry of Education, Science Technology (MEST) and National Research Foundation of Korea (NRF) through the Human Resource Training Project for Regional Innovation.

Literature Cited

1. Xie RJ, Li YQ, Hirosaki N, Yamamoto H. *Nitride Phosphors and Solid-State Lighting*, New York: Taylor and Francis Group, LLC, 2010.
2. Im SG, Gleason KK. Solvent-free modification of surfaces with polymers: the case for initiated and oxidative chemical vapor deposition (CVD). *AIChE J*. 2011;57:276–285.
3. Lefebvre G, Galet L, Chamayou A. Dry coating of talc particles: effect of material and process modifications on their wettability and dispersibility. *AIChE J*. 2011;57:79–86.
4. Purcar V, Stamatin I, Cinteza O, Petcu C, Raditoiu V, Ghiurea M, Miclaus T, Andronie A. Fabrication of hydrophobic and antireflective coatings based on hybrid silica films by sol-gel process. *Surf Coat Technol*. 2012;206:4449–4454.
5. Lee K, Jur JS, Kim DH, Parsons GN. Mechanisms for hydrophilic/hydrophobic wetting transitions on cellulose cotton fibers coated using Al2O3 atomic layer deposition. *J Vac Sci Technol*. 2012;A30: 01A163–01A169.
6. Fang Z, Qiu X, Qiu Y, Kuffel E. Dielectric barrier discharge in atmospheric air for glass-surface treatment to enhance hydrophobicity. *IEEE Trans Plasma Sci*. 2006;34:1216–1221.
7. Lee KH, Cho SC, Jo SY, Uhm HS, Bang CU, Lee DK. Hydrophobic coating of Y2O3:Eu phosphors by using HMDSO/Toluene plasma at low pressure and their wettability. *J Korean Phys Soc*. 2008;53:631–635.
8. Jo SY, Cho SC, Lee KH, Uhm HS. Hydrophobic coating of multi-walled carbon nanotubes by using a HMDSO glow plasma under low pressure. *J Korean Phys Soc*. 2008;53:641–645.
9. Topala I, Asandulesa M, Spridon D, Dumitrascu N. Hydrophobic coating obtained in atmospheric plasma. *IEEE Trans Plasma Sci*. 2009;37:946–950.
10. Kakiuchi H, Ohmi H, Yamada T, Yokoyama K, Okamura K, Yasutake K. Silicon oxide coatings with very high rates (>10 nm/s) by hexamethyldisiloxane-oxyen fed atmospheric-pressure VHF plasma: film-forming behavior using cylindrical rotary electrode. *Plasma Chem Plasma Proc*. 2012;32:533–545.
11. Buyle G, Schneider J, Walker M, Akishev Y, Napartovich A, Perucca M. Plasma systems for surface treatment. In: Rauscher H, Perucca M, Buyle G, editors. *Plasma Technology for Hyperfunctional Surfaces*. Weinheim, Germany: Wiley-VCH, 2010:33–61.
12. Fridman A. *Plasma Chemistry I*, 1st ed. New York: Cambridge University Press, 2008.
13. Yao S, Okumoto M, Madokoro K, Yashima T, Suzuki E. Pulsed dielectric barrier discharge reactor for diesel particulate matter removal. *AIChE J*. 2004;50:1901–1907.
14. Yao S, Madokoro K, Fushimi C, Fujioka Y. Experimental investigation on diesel PM removal using uneven DBD reactors. *AIChE J*. 2007;53 Leei:1891–1897.
15. Morent R, Geyter N, Vlierberghe S, Dubruel P, Leys C, Schacht E. Organic-inorganic behavior of HMDSO films plasma-polymerized at atmospheric pressure. *Surf Coat Technol*. 2009;203: 1366–1372.
16. Vogelsang A, Ohl A, Foest R, Schrder K, Weltmann KD. Hydrophobic coating deposited with an atmospheric pressure microplasma jet. *J Phys D: Appl Phys*. 2010;43:485201.
17. Su K, DeGroot VJ, Norris WA, Lo YP. Siloxane materials for optical applications. *Proc SPIE*. 2006;6029:60291C-1–60291C-8.
18. DeGroot VJ Jr., Norris MA, Glover OS, Clapp VT. Highly transparent silicone materials. *Proc SPIE*. 2004;5517:116–123.
19. Gaur S, Vergason G. Plasma polymerization: theory and practice. In: Proceedings of 43rd Annual Technical Conference, Denver, 2000; 267–271.
20. Theelen M, Habets D, Staemmler L, Winands H, Bolt P. Localised plasma deposition of organosilicon layers on polymer substrates. *Surf Coat Technol*. 2012;211:9–13.
21. Lee JH, Kim YJ. A correlation between a phase transition and luminescent properties of Sr2SiO4:Eu2 + prepared by a flux method. *J Ceram Proc Res*. 2009;10:81–84.
22. Hillborg HC. Loss and recovery of hydrophobicity of polydimethylsiloxane after exposure to electrical discharges. Ph.D. thesis. Royal Institute of Technology, 2001.
23. Yasuda H, Sharma AK. Effect of orientation and mobility of polymer molecules at surfaces on contact angle and its hysteresis. *J Polym Sci Polym Phys Ed*. 1981;19:1285–1291.
24. Kim J, Kim TH, Oh JG, Noh SH, Lee JS, Park KH, Ha S, Kang H. Characterization of acetylene plasma-polymer films: recovery of surface hydrophobicity by aging. *Bull Korean Chem Soc*. 2009;30: 2589–2594.
25. Amin M, Akbar M, Amin S. Hydrophobicity of silicone rubber used for outdoor insulation (an overview). *Rev Adv Mater Sci*. 2007;16: 10–26.
26. David A, Puydt Y, Dupuy L, Descours S, Sommer F, Tran MD, Viard J. Surface analysis for plasma treatment characterization. In: Rauscher H, Perucca M, Buyle G, editors. *Plasma Technology for*

Hyperfunctional Surfaces. Weinheim, Germany: Wiley-VCH, 2010: 91–132.
27. Qiao Y, Zhang X, Ye X, Chen Y, Guo H. Photoluminescent properties of Sr2SiO4:Eu3+ and Sr2SiO4:Eu2+ phosphors prepared by solid-state reaction method. *J Rare Earths*. 2009;27: 323–326.
28. Smith W. *Modern Optical Engineering*, 3rd ed. New York: McGraw-Hill, 2000.
29. Roualdes S, Lee AV, Berjoan R, Sanchez J, Durand J. Gas separation properties of organosilicon plasma polymerized membranes. *AIChE J*. 1999;45:1566–1575.
30. Nishikida K, Coates J. Infrared and Raman analysis of polymers. In: Lobo H, Bonilla J, editors. *Handbook of Plastics Analysis*. New York: Marcel Dekker, Inc., 2003:186–316.

Manuscript received Apr. 20, 2013, and revision received Nov. 1, 2013.